Journal of Power Sources 215 (2012) 122–129

Contents lists available at SciVerse ScienceDirect

Journal of Power Sources

journal homepage: www.elsevier.com/locate/jpowsour

A novel 2,7-diaminofluorene-based organic dye for a dye-sensitized solar cell

Lu-Yin Lin [a], Chuan-Pei Lee [a], Min-Hsin Yeh [a], Abhishek Baheti [b], R. Vittal [a], K.R. Justin Thomas [b], Kuo-Chuan Ho [a,c,*]

[a] Department of Chemical Engineering, National Taiwan University, Taipei 10617, Taiwan
[b] Department of Chemistry, Indian Institute of Technology Roorkee, Roorkee 247 667, India
[c] Institute of Polymer Science and Engineering, National Taiwan University, Taipei 10617, Taiwan

HIGHLIGHTS

► A dye-sensitized solar cell (DSSC) was fabricated with a novel 2,7-Diaminofluorene-based organic dye (JD2).
► TiO_2 film thickness, dye-soaking times, coadsorbate and additives in electrolytes are investigated for JD2-sensitized DSSCs.
► The optimized DSSC shows an efficiency of 6.31%, which is competitive to that of the D149-sensitized cell (7.01%).
► The incident photon-to-current conversion efficiency is much higher in shorter wavelength range of a JD2-sensitized DSSC.
► The longer electron lifetime of a JD2-sensitized DSSC is in consistency with its higher V_{OC}.

GRAPHICAL ABSTRACT

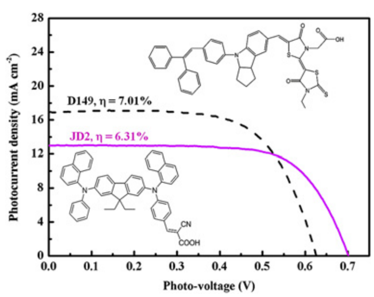

ARTICLE INFO

Article history:
Received 19 December 2011
Received in revised form
6 March 2012
Accepted 26 April 2012
Available online 6 May 2012

Keywords:
Coadsorbate
Dye-sensitized solar cell
JD2 dye
Laser-induced photo–voltage transients
Organic dye

ABSTRACT

A novel 2,7-diaminofluorene-based organic dye (coded as JD2) with the diarylaminofluorene unit as the electron donor and the cyanoacrylic acid as the acceptor as well as anchoring group in a donor-π–donor-π–acceptor architecture is used in a dye-sensitized solar cell (DSSC). The TiO_2 film thickness and the dye soaking time are optimized, and a coadsorbate of bis-(3,3-dimethyl-butyl)-phosphinic acid (DINHOP) is added to the dye solution to reform the cell performance. Effects of the additives, *N*-methyl-benzimidazole (NMBI), guanidinium thiocyanate (GuSCN) or 4-tert-butylpyridine (TBP) in the electrolyte on the photovoltaic performance of the DSSC are studied. Effects of change of DINHOP concentration in JD2 dye solution, change of ratio of LiI to 1,2-dimethyl-3-propylimidazolium iodide (DMPII), and change of concentration of I_2 in the electrolyte on the photovoltaic performance of the DSSC are studied. A light-to-electricity conversion efficiency (η) of 6.31% is achieved for the JD2 dye-based DSSC, which is one of the best efficiencies for a cell with an organic dye. Explanations are made with electrochemical impedance spectra (EIS), laser-induced photo–voltage transients, and incident photo-to-current conversion efficiency (IPCE) curves.

* Corresponding author. Department of Chemical Engineering, National Taiwan University, Taipei 10617, Taiwan. Tel.: +886 2 2366 0739; fax: +886 2 2362 3040.
E-mail addresses: krjt8fcy@iitr.ernet.in (K.R.J. Thomas), kcho@ntu.edu.tw (K.-C. Ho).

0378-7753/$ – see front matter © 2012 Elsevier B.V. All rights reserved.
doi:10.1016/j.jpowsour.2012.04.084

1. Introduction

Dye-sensitized solar cells (DSSCs) have attracted considerable scientific and industrial interest, as promising candidates for renewable energy source, during the past two decades [1,2]. DSSCs based on Ru(II)-polypyridyl complexes, *e.g.*, N3 [3], N719 [4], black dye [5], CYC–B11 [6] etc, as photosensitizers have attained high light-to-electricity conversion efficiencies (η) under AM 1.5 illumination condition. They are economically feasible alternatives to conventional inorganic photovoltaic devices [7,8]. Recently much attention is paid on the DSSCs with metal-free organic dyes, because of their low cost and simple production possibilities, high extinction coefficients of their dyes, and facile molecular design of the dyes. Recently, novel organic dyes based on porphyrin [9,10], perylene [11,12], cyanine [13,14], xanthenes [15,16], merocyanine [17,18], coumarin [19,20], hemicyanine [21,22], indoline [23], diketopyrrolopyrrole [24,25], and ethylenedioxythiophene [26] have been investigated for DSSCs, and significant progress has been made in this field. It is well known that the open-circuit voltage (V_{OC}) of a DSSC is an important factor for the power conversion efficiency of the cell. Charge recombination processes of injected electrons with I_3^- ions in the electrolyte [27,28] and with oxidized dye [29] are considered to be responsible for a low value of the V_{OC}; the value of V_{OC} of a DSSC is presently far below than the theoretical maximum value [30]. A novel organic dye, (*E*)-2-cyano-3-(4-((9,9-diethyl-7-(naphthalene-1-yl(phenyl)amino)-9*H*-fluoren-2-yl)(naphthalen-1-yl)amino)phenyl)acrylic acid (JD2) was recently reported; the dye had the diarylaminofluorene unit as the electron donor and cyanoacrylic acid as the acceptor with anchoring group in a donor-π–donor-π–acceptor architecture [31]. Fig. 1 illustrates the structures of JD2 and D149 dyes, which is a very promising all-organic sensitizer for DSSCs, attracting a continuously growing interest as an alternative system to the commonly used Ru dye [32].

The JD2 dye contains 2,7-fluorenediamine which acts as a cascade donor system. The presence of the additional donor in the molecule is expected to impact the electronic properties of the dye in two ways. One way is its presence lowers the HOMO and thereby increases the chances of dye regeneration, and the other way is that its presence makes the strong visible region absorption of JD2 complementary to that of D149, which occurs at longer wavelength region (>500 nm).

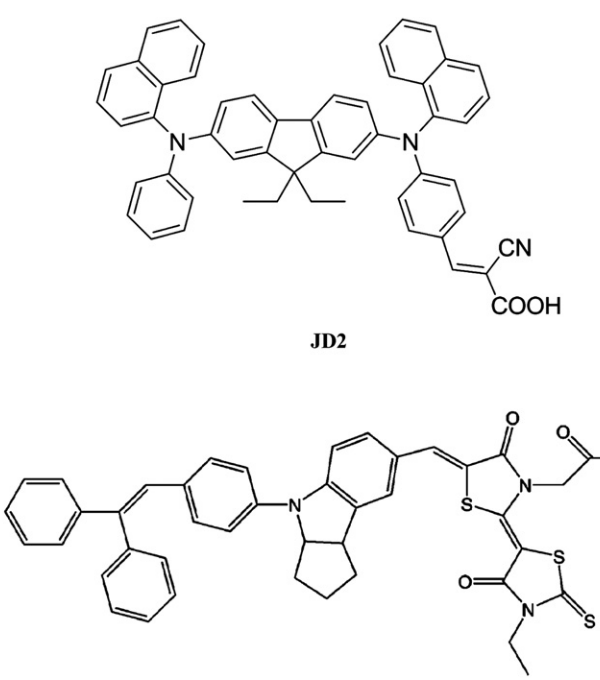

JD2

D149

Fig. 1. Structures of JD2 and D149 dyes.

In this study, the performance of DSSCs sensitized with JD2 dye is investigated. The thickness of the TiO_2 film in the DSSC was controlled, by taking into consideration the surface area of the film and the electron transport length in the film. The dye soaking time was also optimized. A coadsorbate was also included in the dye solution, in order to reduce the recombination current, and its concentration was optimized. Finally, effects of the additives, *N*-methylbenzimidazole (NMBI), guanidinium thiocyanate (GuSCN) or 4-tert-butylpyridine (TBP) in the electrolyte on the photovoltaic performance of the DSSC were studied. With the additive of TBP, the V_{OC} has been improved. The concentration ratio of LiI and DMPII and the amount of I_2 in the electrolyte were also optimized. The best cell efficiency of 6.31% was therefore achieved, with a reference efficiency of 7.01% for a DSSC with D149 dye, which is the most commonly used organic dye in DSSCs. Electrochemical impedance spectroscopy (EIS), incident photon-to-current conversion efficiency (IPCE) curves, and laser-induced photo–voltage transients were employed to substantiate the explanations.

2. Experimental

Lithium iodide (LiI, synthetical grade), iodine (I_2, synthetical grade), and poly(ethylene glycol) (PEG, M.W. ~20,000) were obtained from Merck. *N*-methylbenzimidazole (NMBI, 99%), 4-tert-butylpyridine (TBP, 96%), guanidinium thiocyanate (GuSCN, 99%), and tert-butyl alcohol (tBA, 96%) were obtained from Acros. Titanium tetraisopropoxide (TTIP, >98%), 2-methoxyethanol (≥99.5%), neutral cleaner, and isopropyl alcohol (IPA, 99.5%) were obtained from Aldrich. 3-methoxypropionitrile (MPN, 99%) was obtained from Fluka. Acetonitrile (99.99%) and nitric acid (*ca.* 65% in water) were obtained from J.T. Baker. 1,2-dimethyl-3-propylimidazolium iodide (DMPII > 99.5%) was obtained from Solaronix. Bis-(3,3-dimethyl-butyl)-phosphinic acid (DINHOP) was obtained from Dyesol.

TTIP (72 ml) was added to 0.1 M nitric acid aqueous solution (430 ml) with constant stirring and simultaneous heating to 85 °C for 8 h. When the mixture was cooled down to room temperature, the resultant colloid was transferred to an autoclave (PARR 4540, U.S.A.) and then heated at 240 °C for 12 h to allow a uniform growth of TiO_2 particles (*ca.* 20 nm). Consequently, the TiO_2 colloid was concentrated to 10 wt%. First type of the TiO_2 paste (for a transparent layer) was prepared by adding 25 wt% PEG (with respect to the TiO_2 with particle size of 20 nm) to the above solution. The purpose on the addition of PEG was to control the pore diameters and prevent the film from cracking during a drying process. On the other hand, the second type of the TiO_2 paste (for a scattering layer) was made by incorporating in the above solution 50 wt% of light scattering TiO_2 particles (PT–501A, 100 nm, Ya Chung Industrial Co. Ltd., Taiwan) with respect to normal TiO_2 with particles size of 20 nm. The second type of TiO_2 paste was used to reduce the light loss by back scattering. Fluorine-doped SnO_2 (FTO, TEC-7, ~10 Ω sq^{-1}, NSG America, Inc., NJ, USA) and tin-doped In_2O_3 (ITO, UR-ITO007–0.7 mm, ~10 Ω sq^{-1}, Uni-onward Corp., Taipei, Taiwan) conducting glasses were first cleaned with a neutral cleaner and then washed with deionic water (DI-water), acetone and isopropanol, sequentially. The conducting surface of the FTO was treated with a solution of TTIP in 2-methoxyethanol (weight ratio of 1:3) to obtain a good mechanical contact between the conducting glass and the TiO_2 film, and to isolate the conducting glass surface from the electrolyte as well. A 10 μm thick TiO_2 film

was coated on the treated FTO glass by doctor blade method, and a portion of 0.4 × 4 cm^2 was selected for active area by scrapping the side portions. The as-prepared TiO_2 film was gradually heated to 450 °C in an oxygen atmosphere, and subsequently sintered for 30 min. After annealing and cooling to 80 °C, the TiO_2/FTO photoanode was immersed in a solution with 3 × 0^{-4} M (*E*)-2-cyano-3-(4-((9,9-diethyl-7-(naphthalen-1-yl(phenyl)amino)-9*H*-fluoren-2-yl)(naphthalen-1-yl)amino)phenyl)acrylic acid (JD2) [31] in a mixture of acetonitrile and tert-butyl alcohol (volume ratio of 1:1), at room temperature. The counter electrode (CE) was prepared by sputtering Pt on an ITO substrate (ITO, UR-ITO007–0.7 mm, Unionward Corp., Taiwan, 10 Ω $sq.^{-1}$) which was first cleaned with a neutral cleaner, and then washed with DI-water, acetone and IPA, sequentially. The two electrodes were separated by a 60 μm thick gasket made of ionomer Surlyn (SX1170-25, Solaronix S.A., Aubonne, Switzerland) and then sealed by heating. The electrolyte was injected into the gap between the electrodes by capillarity.

The DSSC was illuminated by a class A quality solar simulator (XES-301S, AM1.5G, San-Ei Electric Co., Ltd., Osaka, Japan) and the incident light intensity (100 mW cm^{-2}) was calibrated with a standard Si Cell (PECSI01, Peccell Technologies, Inc.). The photoelectrochemical characteristics of the DSSC were recorded with a potentiostat/galvanostat (PGSTAT 30, Autolab, Eco-Chemie, the Netherlands). Electrochemical impedance spectra (EIS) were obtained by the above-mentioned potentiostat/galvanostat equipped with an FRA2 module under a constant light illumination of 100 mW cm^{-2}. The frequency range explored was 10 mHz–65 kHz. The bias voltage was set at the open-circuit voltage of the DSSC, between the Pt–CE and the dye/TiO_2/FTO photoanode, starting from the short-circuit condition; the corresponding ac amplitude was 10 mV. The impedance spectra were analyzed using an equivalent circuit model [33,34]. Pulsed laser excitation was applied by a frequency-doubled Q-switched Nd:YAG laser (model Quanta-Ray GCR-3-10, Spectra-Physics Laser) with a 2 Hz repetition rate at 532 nm, and a 7 ns pulse width at half-height. The average electron lifetime could approximately be estimated by fitting a decay of the open-circuit potential transient with exp $(-t\ \tau_e^{-1})$, where t is the time and τ_e is an average time constant before recombination. Incident photo-to-current conversion efficiency (IPCE) curves were obtained at the short-circuit condition. The light source was a class A quality solar simulator (PEC-L11, AM1.5G, Peccell Technologies, Inc.); light was focused through a monochromator (Oriel Instrument, model 74,100) onto the photovoltaic cell.

3. Results and discussion

3.1. Optimization of TiO_2 film thicknesses

The preparation of the TiO_2 film was optimized to elicit high photovoltaic performance from the DSSC. The thickness of the TiO_2 film is one of the important factors to dominantly affect the performance of a DSSC. The photovoltaic performance of the DSSCs with TiO_2 films having thicknesses of 6, 12, 18 and 24 μm are shown in Fig. 2(a), and the corresponding parameters are listed in Table 1. An increase in the cell efficiency (η) from 4.32% to 5.28% can be noticed for the DSSC, when the thickness of TiO_2 film is increased from 6 to 12 μm; further increases in the TiO_2 film thickness, *i.e.*, to 18 and 24 μm cause decreases in the efficiency to 4.38% and 3.81%, respectively. It is generally believed that thicker TiO_2 films can provide more dye molecules to adsorb on them [35,36]. The results indicate that the diffusion length of photo-excited electrons traveling in the TiO_2 particle network is limited to less than around 12 μm. The electron transporting length becomes longer with thicker TiO_2 films, *i.e.*, 18 and 24 μm in this case, which may cause a higher probability of recombination; as a result, the J_{SC} decreases with further increase in the thickness of the TiO_2 film. Thicker TiO_2 films show decreases in V_{OC} for the pertinent DSSCs, which could be attributed to increasing probability of recombination, owing to the longer electron transporting path. The fill factor (FF) decreases with increasing thickness of the TiO_2 film as well, due to the larger series resistance in the thicker TiO_2 film [37]. The results are consistent

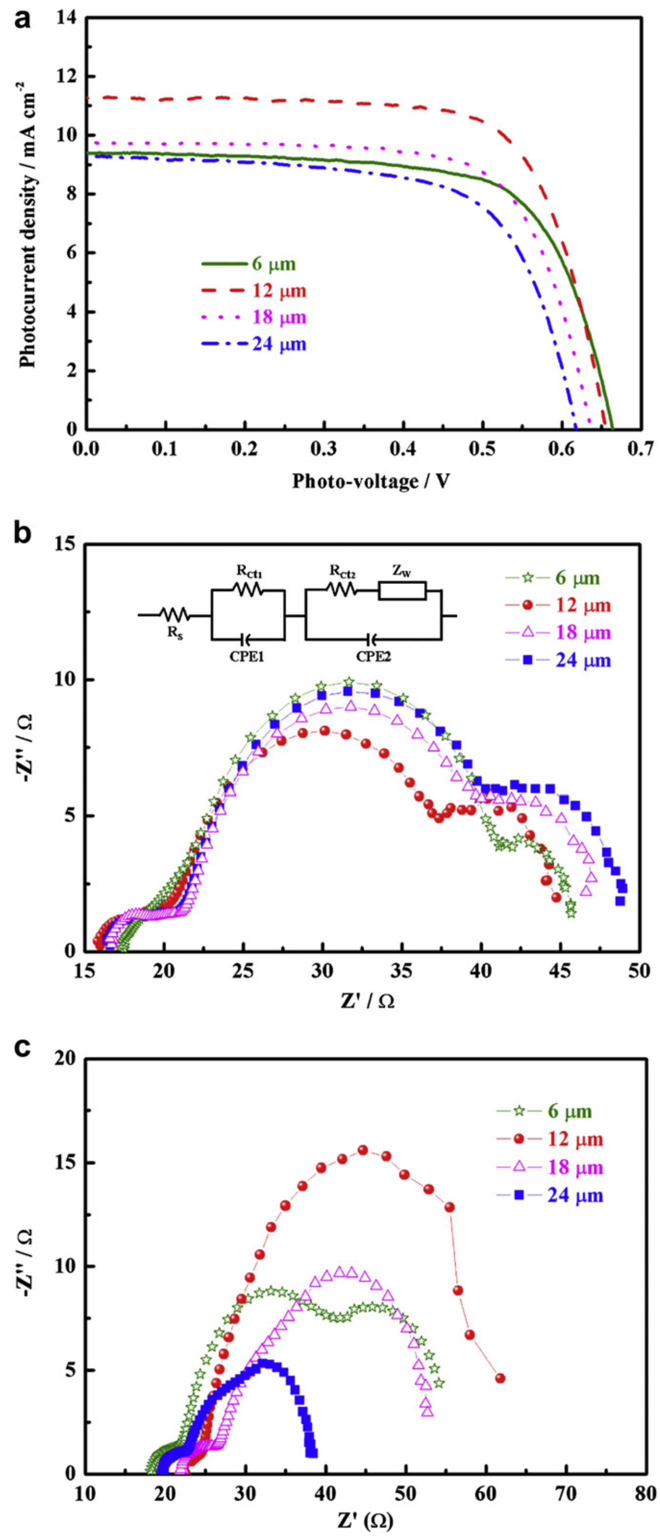

Fig. 2. (a) Photocurrent density–voltage characteristics, (b) EIS spectra of the DSSCs with TiO_2 films of different thicknesses, measured at 100 mW cm^{-2} light intensity, and (c) EIS spectra of the DSSCs with TiO_2 films of different thicknesses, measured in dark.

Table 1
Photovoltaic parameters of the DSSCs with TiO_2 films of different thicknesses, measured at 100 mW cm^{-2} light intensity. The table also shows the corresponding values of the charge transfer resistance, R_{ct2}.

Thickness/μm	V_{OC}/V	J_{SC}/mA cm^{-2}	FF	η (%)	R_{ct1}/Ω	R_{ct2}/Ω
6	0.67	9.38	0.70	4.32	4.22	25.56
12	0.66	11.35	0.72	5.28	4.81	21.67
18	0.64	9.75	0.69	4.38	4.11	24.27
24	0.62	9.74	0.63	3.81	4.19	27.46

with those in our previous report [36]. EIS technique was used to characterize the charge transfer resistances of the cells. Fig. 2(b) shows the Nyquist plots of electrochemical impedance spectra (EIS) spectra of the DSSCs with different thicknesses of TiO_2 film, measured under illumination, and the equivalent circuit is shown in the inset of the figure. The ohmic serial resistance (R_S) in the equivalent circuit corresponds to the overall series resistance. In general, the impedance spectrum of a DSSC, measured under illumination, shows three semicircles in the frequency range of 10 mHz–65 kHz. The first semicircle (R_{ct1}) represents the charge transfer resistances at the counter electrode and the electrolyte, at the electrical contact between the conductive substrate and TiO_2 film, and among the TiO_2 particles [38–40]. The second semicircle (R_{ct2}) corresponds to the charge transfer resistance at the interface between TiO_2/dye/electrolyte. The third semicircle in the low frequency range (1–0.01 Hz) represents the impedance associated with the Warburg diffusion process of I^-/I_3^- in the electrolyte (Z_W). The values of R_{ct1} and R_{ct2} are shown in Table 1. The values of R_{ct1} for all the cases vary to a small extent, indicating similar charge transfer resistances at the counter electrode and the electrolyte, at the electrical contact between the conductive substrate and TiO_2 film, and among the TiO_2 particles [38–40]. The R_{ct2} values increase with increasing thickness of TiO_2 film above 12 μm, resulting in reduced performances of the DSSCs with thicker TiO_2 films, *i.e.*, thicker than 12 μm. We have also measured the EIS at an applied bias of −0.80 V in the dark to elucidate the correlation of electron transport with different thicknesses of TiO_2. In these cells operated in dark, electrons transport through the mesoporous TiO_2, and I^- is oxidized to I_3^- at the counter electrode at the same time [41]. Fig. 2(c) shows the Nyquist plots of the DSSCs with different thicknesses of TiO_2 films, obtained in dark. The largest circles at the middle frequencies represent the recombination resistance, R_{rec}, *i.e.*, the resistance for the direct transfer of electrons from the TiO_2 conduction band to I_3^- at the interface between TiO_2/dye/electrolyte or in the electrolyte [42]. Under dark conditions, larger R_{rec} indicates a smaller charge recombination rate. The largest value of R_{rec} can be noticed for the DSSC with TiO_2 thickness of 12 μm; thus in this case the charge recombination is the least. This is also vindicated by the fact that the optimized thickness of the TiO_2 film for JD2 dye is about 12 μm.

The first, second and third semicircles correspond to the charge transfer resistances at the counter electrode (R_{ct1}), at the TiO_2/dye/electrolyte interface (R_{ct2}) and to the Warburg diffusion process of I^-/I_3^- in the electrolyte (R_{diff}), respectively. The corresponding values of R_{ct2} are shown in Table 1. Apparently, the R_{ct2} increases with increasing thickness of the TiO_2 film above 12 μm. The performances of the DSSCs with thicker TiO_2 films (thicker than 12 μm) are thus reduced owing to their larger charge transfer resistances. The results also confirm that the optimized thickness of the TiO_2 film for JD2 dye is about 12 μm.

3.2. Optimization of the soaking time for TiO_2 films in JD2 dye

On the other hand, because of different sizes of different dye molecules, the soaking time of the TiO_2 film in the dye solution should be controlled to optimize the cell performance. The photocurrent density–voltage curves of the DSSCs with TiO_2 films sensitized with JD2 dye for 3, 6, 12, 24, and 48 h are shown in Figure S1 in the electronic supplementary information, and the corresponding photovoltaic parameters are given in Table S1; the behaviors of J_{SC} and η of these DSSCs as a function of the soaking time are depicted in Fig. 3. It can be seen in Table S1 that the J_{SC} increases with increasing soaking time of the TiO_2 film in JD2 dye, and the highest value of 11.35 mA cm^{-2} is attained for 24 h of soaking; however, it decreases with further increases in the soaking time to 48 h. The results reveal that with the soaking time less than 24 h, the TiO_2 films are not fully adsorbed by the dye molecules; however, when the soaking time is too long, *i.e.*, 48 h, the cell performance decreases, and this decreased cell performance may be due to the desorption of the dye molecules from the TiO_2 film. We have obtained the absorption spectra of the TiO_2 films soaked in JD2 dye for 3, 6, 12, 24, and 48 h to compare the relative amounts of dyes adsorbed on the films, as shown in Figure S2 in the supporting information. It can be seen in the figure that the absorption increases with increasing soaking time of TiO_2 film in JD2 dye until 24 h, and then drastically decreases with increase in the soaking time from 24 h to 48 h. This observation reveals that 24 h is the optimum time for dye adsorption on TiO_2 films, and the increase in soaking time beyond this time causes a desorption of the JD2 dye from the films.

3.3. Investigation of the coadsorbate concentration in JD2 dye

It is now accepted that judiciously designed coadsorbate molecules can reduce the dark currents of a DSSC (under forward bias); the coadsorbate molecules diminish the charge recombination and/or raise the conduction band edge energy level of TiO_2 [43]. Therefore, in order to further improve the cell performance, the coadsorbate DINHOP was added into the JD2 dye, and its concentration effects were investigated on the performance of a DSSC. The coadsorbate of DINHOP was added into the dye solution with the concentration of 9 wt% and 16 wt%; the dye solution without any coadsorbate was also used as a reference. The photovoltaic performance of the DSSCs with different concentrations of DINHOP in JD2 dye solution is illustrated in Fig. 4(a), and the corresponding parameters are listed in Table S2. Clearly, with less addition of DINHOP (9 wt%) into the JD2 dye solution, the V_{OC} and η of the corresponding DSSC are the highest, being 0.69 V and 5.36%, respectively. DINHOP has been demonstrated as an effective

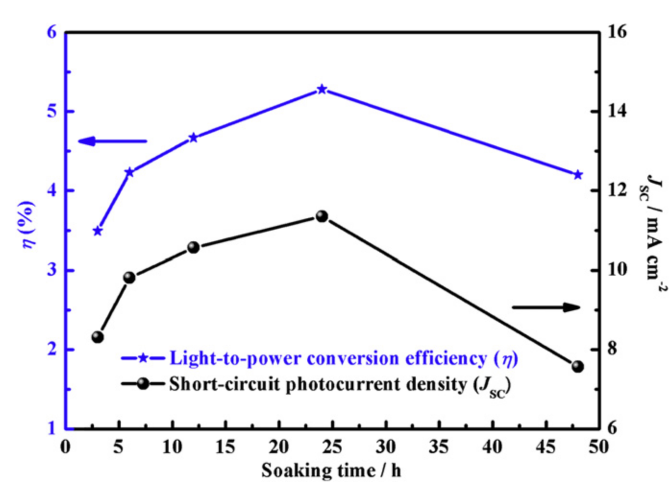

Fig. 3. Behaviors of J_{SC} and η of the DSSCs with TiO_2 films sensitized with JD2 dye for 3, 6, 12, 24, and 48 h as functions of the soaking time.

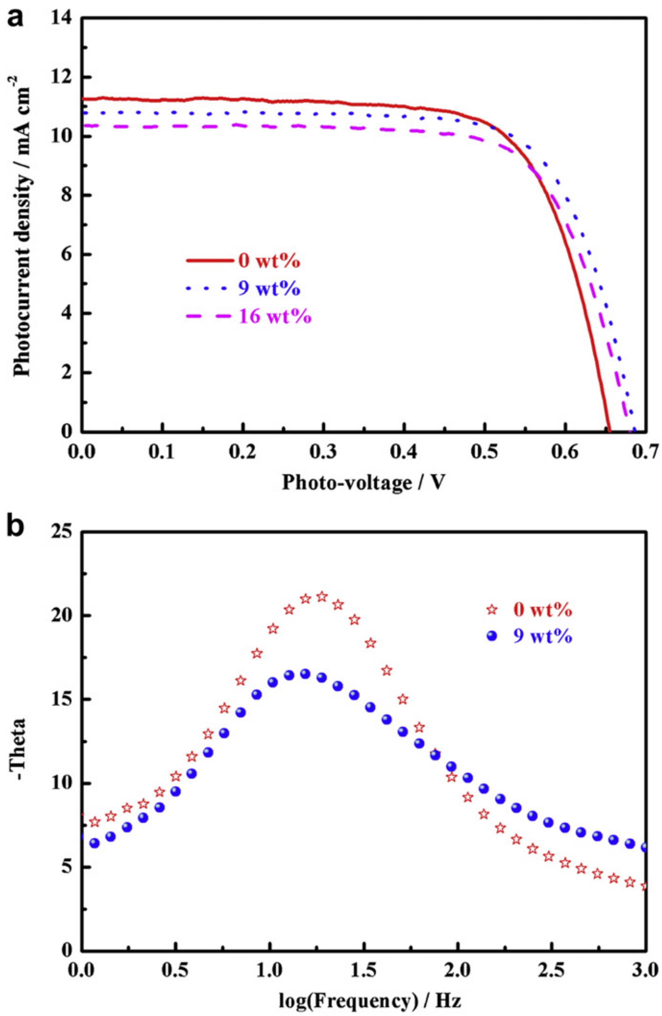

Fig. 4. (a) Photocurrent density–voltage characteristics of the DSSCs with different concentrations of the coadsorbent (DINHOP) in JD2 dye solution, measured at 100 mW cm^{-2} light intensity; (b) Bode phase plots of the DSSCs with different concentrations of the coadsorbent (DINHOP) in JD2 dye solution, obtained at 100 mW cm^{-2} light intensity under open-circuit voltage.

coadsorbate for reducing the dark current, due to a retardation of interfacial recombination of photo-generated charge carriers [6]; this is the reason for the improved V_{OC} with the addition of DINHOP. However, the dye concentration on the TiO_2 surface is expected to reduce with the increase in the amount of DINHOP in the dye solution [43]; this is probably the reason for the reduced cell efficiency of 5.05% with increased amount of DINHOP in the JD2 dye solution (16 wt%). Fig. 4(b) shows Bode phase plots of the DSSCs with different concentrations of the coadsorbent (DINHOP) in JD2 dye solution. The electron lifetimes (τ_e) in the JD2 dye-sensitized TiO_2 films with the addition of DINHOP (9 wt%) and without its addition were determined from the Bode phase plots, as shown in Fig. 4(b), using Eqn. (1) as following,

$$\tau_e = \frac{1}{2\pi f_{max}} \tag{1}$$

where f_{max} is the frequency value of characteristic low-frequency peak in the plot. A longer τ_e was found for the TiO_2 film with the presence of DINHOP in the dye solution, which has smaller f_{max} than that of the film without DINHOP in its dye solution. The result is in consistency with the higher V_{OC} of the DSSCs with DINHOP added as the coadsorbate into the JD2 dye solution (Table S2).

3.4. Effects of additives in the electrolyte

It is to be noticed here that the composition of the electrolyte used in the previous experiment is 0.1 M LiI, 0.6 M DMPII, 0.05 M I_2 and 0.5 M TBP in a mixture of ACN/MPN (volume ratio of 1:1). We next examined the effects of other additives in the electrolyte on the performance of a DSSC. Fig. 5(a) shows photovoltaic performance of the DSSCs with 0.5 M of NMBI or GuSCN or TBP as the additive in the electrolyte, and the corresponding parameters are listed in Table S3; the figure also shows the performance of the DSSC without any additive in its electrolyte (0.1 M LiI, 0.6 M DMPII and 0.05 M I_2). Improvements in the V_{OC} values can be noticed in the case of presence of any of the additives in the electrolyte, with reference to the V_{OC} value of the cell without any additive. The best η of 5.36% was achieved for the DSSC with TBP as the additive in the electrolyte, which also shows the highest V_{OC} of 0.69 V. Moreover, the electron lifetimes (τ_e) were determined in the TiO_2 films of the DSSCs with and without TBP in the electrolyte, by a laser-induced photo–voltage transient technique; the corresponding curves are shown in Fig. 5(b). The value of τ_e could approximately be estimated by fitting a decay of the open circuit voltage transient with $\exp(-t\,\tau_e^{-1})$, where t is the time and τ_e is an average time constant before recombination. The values of τ_e were found to be 0.54 and

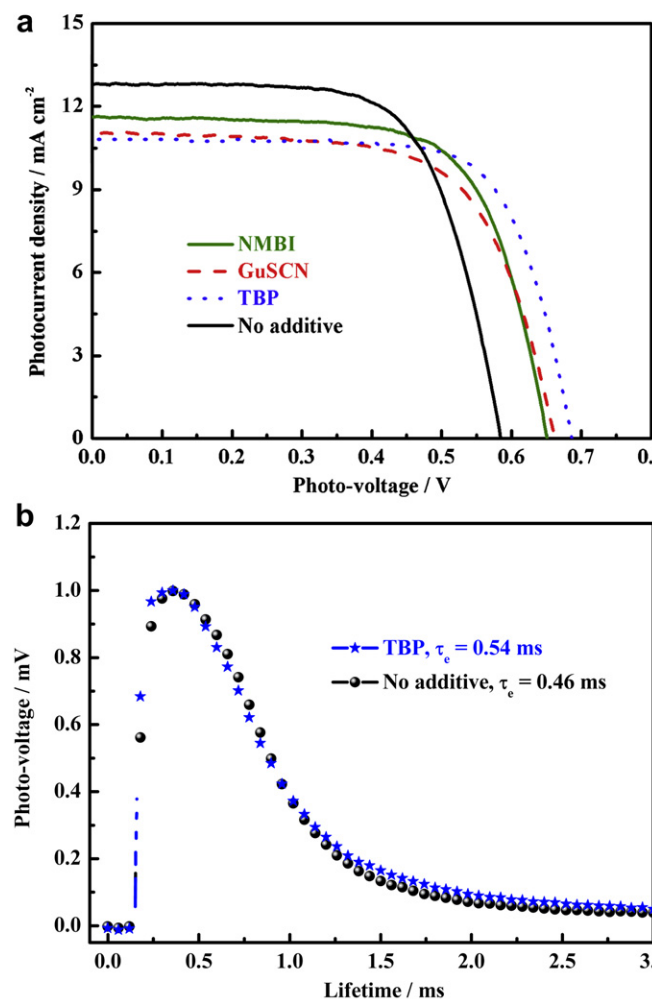

Fig. 5. (a) Photovoltaic performance of the DSSCs with 0.5 M of NMBI or GuSCN or TBP as the additive, and without any additive in the electrolyte, measured at 100 mW cm^{-2} light intensity; (b) Transient photo–voltage curves of the DSSCs with TBP as the additive in the electrolyte and without any additive in the electrolyte.

0.46 ms for the DSSCs with and without TBP in their electrolytes, respectively. The higher value of τ_e for the TiO_2 film for the cell with TBP is in consistency with its higher value of V_{OC} (Table S3), which can be attributed to the back electron transfer suppression at the TiO_2-electrolyte interface and to the shift of the potential of conduction band edge of TiO_2 to a negative level [44].

3.5. Effects of concentration ratios of LiI to 1,2-dimethyl-3-propylimidazolium iodide in the electrolyte

It was demonstrated that cations with large sizes tend to cause a high reductive activity of I^- and a low diffusion coefficient of I_3^- [45]. Therefore, the effects of concentration ratios of LiI to DMPII in the electrolyte were investigated on the photovoltaic performance of a DSSC; the concentration of I^- was fixed to be 0.7 M in all these cases. The photovoltaic parameters of the DSSCs with different concentration ratios of LiI to DMPII in their electrolytes are listed in Table 2, and the corresponding photocurrent density–voltage curves are shown in Figure S2. The concentrations of LiI and DMPII in the electrolytes were: 0.6 M LiI + 0.1 M DMPII and 0.1 M LiI + 0.6 M DMPII. Two electrolytes with only LiI or DMPII were also investigated. All the electrolytes contained the common composition of 0.05 M I_2 and 0.5 M TBP in a mixture of ACN/MPN (volume ratio of 1:1). As shown in Figure S2 and Table 2, the V_{OC} of a cell increases with the increase of concentration of DMPII. The cell with only DMPII, *i.e.*, without any LiI shows the highest value of 0.80 V; however, the cell efficiency is not the highest in this case, because of its lowest J_{SC} (8.00 mA cm^{-2}), which was probably caused by a slow diffusion of DMPII ions in the electrolyte due to their large cation size. The large size of DMPII results in a low mass transfer rate of $DMPI^+$ ions in the electrolyte, which in turn causes a small J_{SC} for its cell [46,47]. On the other hand, higher J_{SC} is observed with higher concentration of LiI, which is apparently due to faster diffusion of Li^+ ions in the electrolyte, which in turn is due to its small size; however, the V_{OC} decreases with increase in the concentration of Li^+, because the potential of TiO_2 conduction band shifts positively due to the positive charge of Li^+ ions adsorbing on the TiO_2 surface [48,49]. As a result, even with the highest value of J_{SC} (12.13 mA cm^{-2}), the cell with 0.7 M of LiI in its electrolyte shows the least η value of 4.85%, because of its least value of V_{OC} (0.60 V). The DSSC with 0.1 M LiI and 0.6 M DMPII in its electrolyte shows the best performance, with V_{OC} of 0.69 V, J_{SC} of 10.81 mA cm^{-2}, FF of 0.72, and η of 5.36%.

3.6. Effect of iodide concentration in the electrolyte

It is well known that I_2 exists in the electrolyte with I^- ions in the form of polyiodides such as I_3^- or I_5^- [50,51]. An efficient transport of I^- ions in the electrolyte is necessary for good performance of a DSSC, because the oxidized dye should be regenerated by I^- ion efficiently after the electrons from the excited state of the dye are injected into the conduction band of TiO_2 under illumination. An efficient transport of I_3^- ions in the electrolyte is also equally important, because in absence of such a transport, and thereby in absence of an efficient transfer of electrons from the CE to I_3^- ions, the electrons accumulated at the CE through the external circuit would lead to a concentration overpotential at the CE and thereby a loss of energy for the DSSC. At the same time, an increasing content of I_2 or I_3^- leads to enhanced light absorption by the electrolyte even in the visible range [52]. In addition, excessive I_2 would increase the dark reduction current [53]. Therefore, it is important to optimize the concentration of I_2 in the electrolyte. Fig. 6 illustrates the photocurrent density–voltage curves of the DSSCs with 0.1 M LiI, 0.6 M DMPII, 0.5 M TBP and different concentrations of I_2 in the electrolytes, measured at 100 mW cm^{-2} light intensity and in the dark; the corresponding photovoltaic parameters are presented in Table 3. The table also shows the ionic conductivities of the corresponding electrolytes. A higher cell efficiency of 6.31% is obtained for the DSSC with 0.03 M I_2 in the electrolyte, compared to that of the cell with 0.05 M I_2 in the electrolyte (5.36%). Obviously, the J_{SC} is highest at the I_2 concentration of 0.03 M, and decreases with further increase in the concentration of I_2; the η shows the same tendency as well. It was reported that the dark current density or the recombination reaction rate increases with increasing concentration of I_2 [53,54]; the values of V_{OC} in Table 3 are in consistency with this report. Ionic conductivities (σ_S) of the electrolytes with 0.1 M LiI, 0.6 M DMPII, 0.5 M TBP and different concentrations of I_2 were calculated by using Eqn. (2) as following,

$$\sigma_S = \frac{d_s}{A_s R_s} \tag{2}$$

The ohmic serial resistances (R_s) of the electrolytes, along with that of a standard solution of NaCl (with a known conductivity of 12.9 mS cm^{-1}, Model 011,006, Thermo Orion) were experimentally measured from Nyquist plots (Pt/electrolyte/Pt); obtaining first the value of d_s/A_s from the known σ_S and R_S values of NaCl, the conductivities of other electrolytes were calculated using their measured R_S values. It is clear in the table that the ionic conductivity increases with increasing concentration of I_2; this increased ionic conductivity has probably increased the J_{SC} at the initial stage of increase of concentration of I_2 (from 0.02 M to 0.03 M); further increase in the concentration of I_2 is associated not only with the increase in conductivity, but also with an increase in the light

Table 2
Photovoltaic parameters of the DSSCs with different concentrations of LiI and DMPII in their electrolytes, measured at 100 mW cm^{-2} light intensity; the table also shows the parameters of the cells with only LiI or DMPII; the concentration of I^- in the electrolytes was fixed to be 0.7 M in all these cases.

Concentration of LiI and DMPII	V_{OC}/V	J_{SC}/mA cm^{-2}	FF	η (%)
0.7 M LiI	0.60	12.13	0.67	4.85
0.6 M LiI + 0.1 M DMPII	0.68	11.62	0.71	5.05
0.1 M LiI + 0.6 M DMPII	0.69	10.81	0.72	5.36
0.7 M DMPII	0.80	8.00	0.75	3.79

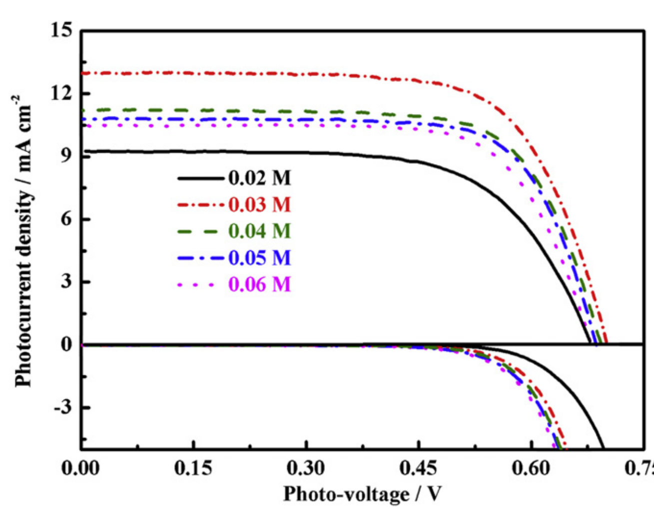

Fig. 6. Photocurrent density–voltage characteristics of the DSSCs with 0.1 M LiI, 0.6 M DMPII, 0.5 M TBP and different concentrations of I_2, measured at 100 mW cm^{-2} light intensity and in the dark.

Table 3
Photovoltaic parameters of the DSSCs with 0.1 M LiI, 0.6 M DMPII, 0.5 M TBP and different concentrations of I_2, measured at 100 mW cm^{-2} light intensity. The ionic conductivities of corresponding electrolytes are also listed in the table.

Concentration of I_2/M	V_{OC}/V	J_{SC}/mA cm^{-2}	FF	η (%)	σ_S/mS cm^{-1}
0.02	0.68	9.25	0.65	4.11	10.14
0.03	0.71	13.00	0.69	6.31	10.32
0.04	0.69	11.19	0.71	5.51	10.45
0.05	0.69	10.81	0.72	5.36	10.60
0.06	0.68	8.30	0.71	5.07	11.43

absorption by the electrolyte. The detrimental effect of light absorption by the electrolyte has possibly nullified the beneficial effect of increase in conductivity of the electrolyte at higher concentrations of I_2, and this may be the reason that the J_{SC} has rather decreased with the increase in the concentration of I_2 beyond the limit of 0.03 M. Increased concentration of I_2 leads to increased concentration of I_3^- ions, and thereby to increased availability of I_3^- ions for recombination, *i.e.*, to a decrease in V_{OC} and J_{SC}; this may be another reason for the decreases in J_{SC}, in spite of increases in conductivity at higher concentrations of I_2.

3.7. Performances of the dye-sensitized solar cells with JD2 and D149 dye

The optimized performance of the DSSC with JD2 dye was achieved with 12 μm of TiO_2 film, 24 h of soaking in JD2 dye solution, DINHOP as the coadsorbate with the concentration of 9 wt % in JD2 dye, and with 0.1 M LiI, 0.6 M DMPII, 0.03 M I_2, and 0.5 M TBP in a mixture of ACN/MPN (volume ratio of 1:1) as the electrolyte. A highly light-absorbing indolene-based dye, termed D149 [55] was also used, at the same conditions as those of JD2 dye, and the photovoltaic parameters were recorded to make a comparative study between the performances of the DSSCs with these two dyes. Fig. 7(a) shows the photocurrent density–voltage curves of the DSSCs with JD2 and D149 dyes, measured at 100 mW cm^{-2} light intensity, and Table 4 gives the corresponding photovoltaic parameters. A cell efficiency of 6.31% is achieved for the DSSC with our synthesized JD2 dye, which is one of the best efficiencies of DSSCs sensitized with organic dyes; as a comparison, the cell with the organic dye D149 shows an efficiency of 7.01%. Fig. 7(b) shows the EIS spectra of the DSSCs with JD2 and D149 dyes, and the corresponding values of R_{ct2} are also listed in Table 4. From Fig. 7(b), it is clear that the charge transfer resistance of the DSSC with JD2 dye is larger than that with D149 dye; the difference, however, is small. Also, the IPCE behavior of the DSSCs was investigated, and the spectra are shown in Fig. 7(c). It can be seen in Fig. 7(c) that the JD2 dye mainly absorbs the sunlight in the wavelength range lower than 500 nm, and the IPCE values in this range are much higher for the cell with this dye than those of the cell with D149 dye; however, above this wavelength limit (500 nm) the cell with D149 dye shows higher IPCE values than those of the cell with JD2 dye. Absorption spectra of the dyes JD2 and D149 are shown in Figure S3. The JD2 dye absorbs the light mainly in the shorter wavelength region, while the D149 dye absorbs it in the longer wavelength region. The D149 dye shows absorption in a broader range of wavelength than that for JD2 dye, resulting in a higher J_{SC} for the cell with D149 dye. The IPCE curves also clearly show that the integrated area under the curve of D149 dye is much higher than that under the curve of JD2 dye. In other words, the photon-to-current conversion efficiency is higher in the case of D149 dye. Furthermore, transient photo–voltage curves of the DSSCs with JD2 and D149 dye are shown in Fig. 7(d). The electron lifetimes could approximately be estimated by fitting a decay of the open-circuit voltage transient with exp $(-t\ \tau_e^{-1})$, where t is the time and τ_e is an average time constant before recombination. The values of τ_e were found to be 0.61 and 0.29 ms for the photoanodes sensitized with JD2 and D149 dyes, respectively. The higher value of τ_e for the DSSC with JD2 dye is in consistency with the higher V_{OC} of the cell (Table 4).

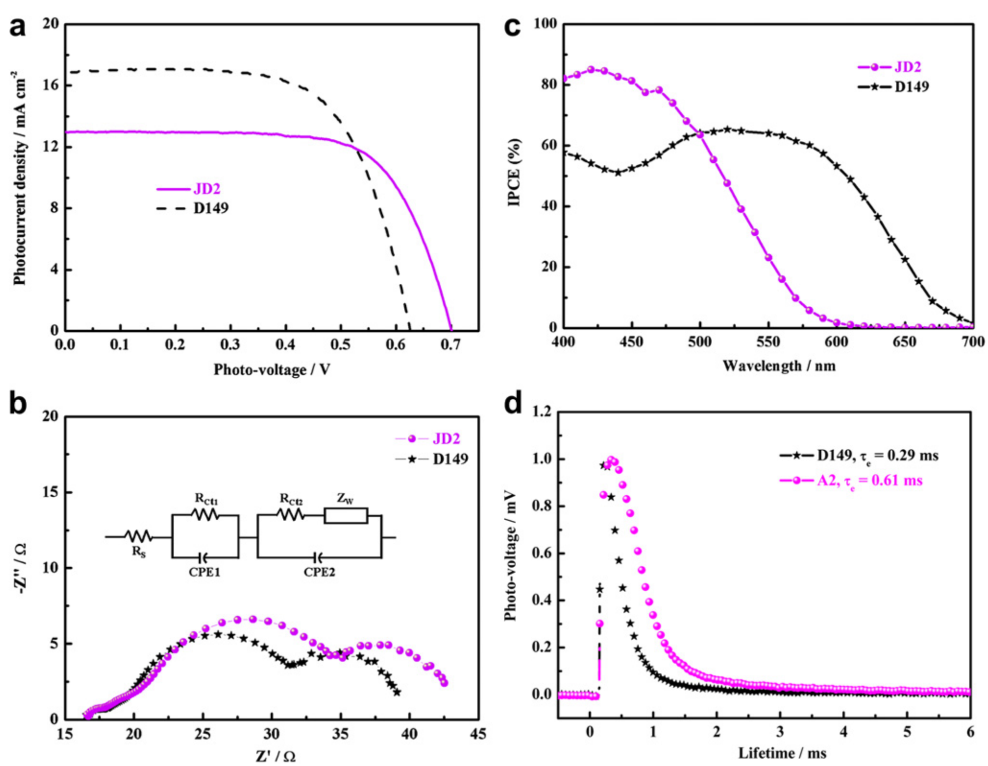

Fig. 7. (a) Photocurrent density–voltage curves and (b) EIS spectra of the DSSCs with JD2 and D149 dyes, measured at 100 mW cm^{-2} light intensity; (c) IPCE spectra and (d) Transient photo–voltage curves of the DSSCs with JD2 and D149 dyes.

Table 4
Photovoltaic parameters of the DSSCs with JD2 and D149 dyes, measured at 100 mW cm^{-2} light intensity. The table also shows the corresponding values of charge transfer resistance, R_{ct2}.

Dye	V_{OC}/V	J_{SC}/mA cm^{-2}	FF	η (%)	R_{ct2}/Ω
JD2	0.71	13.00	0.69	6.31	18.86
D149	0.63	16.94	0.66	7.01	15.60

4. Conclusions

A dye-sensitized solar cell (DSSC) was fabricated with a novel 2,7-diaminofluorene-based organic dye (JD2). The cell shows the highest light-to-power conversion efficiency (η) when the thickness of its TiO_2 film is 12 μm, the concentration ratio between LiI and 1,2-dimethyl-3-propylimidazolium iodide (DMPII) is 1:6, the concentration of I_2 is 0.03 M, the dye (JD2) soaking time is 24 h, and when the concentration of the coadsorbate bis-(3,3-dimethylbutyl)-phosphinic acid (DINHOP) is 9 wt%. Among *N*-methylbenzimidazole (NMBI), guanidinium thiocyanate (GuSCN), and 4-tert-butylpyridine (TBP) in the electrolyte of a DSSC, the last one rendered the best η for the cell. The optimized DSSC showed η of 6.31%, which is competitive to that of the cell with D149 dye (7.01%). The IPCE values of the DSSC with JD2 dye are much higher than those of the cell with D149 dye in the wavelength range below 500 nm; however, above this wavelength limit (500 nm) the cell with D149 dye shows higher IPCE values than those of the cell with JD2 dye. The JD2 dye absorbs the light mainly in the shorter wavelength region, while the D149 dye absorbs it in the longer wavelength region. The higher value of τ_e of the DSSC with JD2 dye (0.69 ms) than that of the DSSC with D149 dye (0.61 ms) is in consistency with its higher value of V_{OC} (0.71 V).

Acknowledgements

This work was supported in part by the National Research Council of Taiwan under grant numbers NSC 98-3114-E-008-002 and NSC 100-3113-E-008-003. Some of the instruments used in this study were made available through the financial support of the Academia Sinica, Taipei, Taiwan, under grant AS-100-TP-A05.

Appendix A. Supplementary material

Supplementary data associated with this article can be found, in the online version, at doi:10.1016/j.jpowsour.2012.04.084.

References

[1] L.M. Goncalves, V. De Zea Bermudez, H.A. Ribeiro, A.M. Mendes, Energy Environ. Sci. 1 (2008) 655–667.
[2] M. Grätzel, Acc. Chem. Res. 42 (2009) 1788–1798.
[3] R.J. Ellingson, J.B. Asbury, S. Ferrere, H.N. Ghosh, J.R. Sprague, T. Lian, A.J. Nozik, J. Phys. Chem. B 102 (1998) 6455–6458.
[4] M.K. Nazeeruddin, R. Splivallo, P. Liska, P. Comte, M. Grätzel, Chem. Commun. 9 (2003) 1456–1457.
[5] M.K. Nazeeruddin, P. Péchy, M. Grätzel, Chem. Commun. (1997) 1705–1706.
[6] C.Y. Chen, M. Wang, J.Y. Li, N. Pootrakulchote, L. Alibabaei, C.H. Ngoc Le, J.D. Decoppet, J.H. Tsai, C. Grätzel, C.G. Wu, S.M. Zakeeruddin, M. Grätzel, ACS Nano 3 (2009) 3103–3109.
[7] P. Wang, S.M. Zakeeruddin, J.E. Moser, M.K. Nazeeruddin, T. Sekiguchi, M. Grätzel, Nat. Mater. 2 (2003) 402–407.
[8] D. Shi, N. Pootrakulchote, R. Li, J. Guo, Y. Wang, S.M. Zakeeruddin, M. Grätzel, P. Wang, J. Phys. Chem. C 112 (2008) 17046–17050.
[9] C.Y. Lee, J.T. Hupp, Langmuir 26 (2010) 3760–3765.
[10] H. Imahori, Y. Matsubara, H. Iijima, T. Umeyama, Y. Matano, S. Ito, M. Niemi, N.V. Tkachenko, H. Lemmetyinen, J. Phys. Chem. C 114 (2010) 10656–10665.
[11] C. Li, Z. Liu, J. Schöneboom, F. Eickemeyer, N.G. Pschirer, P. Erk, A. Herrmann, K. Müllen, J. Mater. Chem. 19 (2009) 5405.
[12] Y. Jin, J. Hua, W. Wu, X. Ma, F. Meng, Synth. Met. 158 (2008) 64–71.
[13] W. Wu, J. Hua, Y. Jin, W. Zhan, H. Tian, Photochem. Photobio. Sci. 7 (2008) 63.
[14] X. Ma, J. Hua, W. Wu, Y. Jin, F. Meng, W. Zhan, H. Tian, Tetrahedron 64 (2008) 345–350.
[15] S. Hattori, T. Hasobe, K. Ohkubo, Y. Urano, N. Umezawa, T. Nagano, Y. Wada, S. Yanagida, S. Fukuzumi, J. Phys. Chem. B 108 (2004) 15200–15205.
[16] J.R. Mann, M.K. Gannon, T.C. Fitzgibbons, M.R. Detty, D.F. Watson, J. Phys. Chem. C 112 (2008) 13057–13061.
[17] K. Sayama, K. Hara, H. Sugihara, H. Arakawa, N. Mori, M. Satsuki, S. Suga, S. Tsukagoshi, Y. Abe, Chem. Commun. (2000) 1173–1174.
[18] K. Sayama, S. Tsukagoshi, T. Mori, K. Hara, Y. Ohga, A. Shinpou, Y. Abe, S. Suga, H. Arakawa, Sol. Energy Mater. Sol. Cells 80 (2003) 47–71.
[19] K. Hara, K. Sayama, H. Arakawa, Y. Ohga, A. Shinpo, S. Suga, Chem. Commun. (2001) 569–570.
[20] Z.S. Wang, Y. Cui, Y. Dan-Oh, C. Kasada, A. Shinpo, K. Hara, J. Phys. Chem. C 111 (2007) 7224–7230.
[21] Y.S. Chen, C. Li, Z.H. Zeng, W.B. Wang, X.S. Wang, B.W. Zhang, J. Mater. Chem. 15 (2005) 1654.
[22] Z.S. Wang, F.Y. Li, C.H. Huang, Chem. Commun. (2000) 2063–2064.
[23] W.H. Howie, F. Claeyssens, H. Miura, L.M. Peter, J. Am. Chem. Soc. 130 (2008) 1367–1375.
[24] F. Guo, S. Qu, W. Wu, J. Li, W. Ying, J. Hua, Synth. Met. 160 (2010) 1767–1773.
[25] S. Qu, W. Wu, J. Hua, C. Kong, Y. Long, H. Tian, J. Phys. Chem. C 114 (2010) 1343–1349.
[26] W. Zeng, Y. Cao, Y. Bai, Y. Wang, Y. Shi, M. Zhang, F. Wang, C. Pan, P. Wang, Chem. Mat. 22 (2010) 1915–1925.
[27] Z. Ning, Q. Zhang, H. Pei, J. Luan, C. Lu, Y. Cui, H. Tian, J. Phys. Chem. C 113 (2009) 10307–10313.
[28] Z. Ning, Y. Fu, H. Tian, Energy Environ. Sci. 3 (2010) 1170–1181.
[29] J.E. Kroeze, N. Hirata, S. Koops, M.K. Nazeeruddin, L. Schmidt Mende, M. Grätzel, J.R. Durrant, J. Am. Chem. Soc. 128 (2006) 16376–16383.
[30] F. De Angelis, S. Fantacci, A. Selloni, M. Grätzel, M.K. Nazeeruddin, Nano Lett. 7 (2007) 3189–3195.
[31] A. Baheti, P. Singh, C.P. Lee, K.R.J. Thomas, K.C. Ho, J. Org. Chem. 76 (2011) 4910–4920.
[32] E. Guillén, J. Idígoras, T. Berger, J.A. Anta, C. Fernández Lorenzo, R. Alcántara, J. Navas, J. Martín Calleja, Phys. Chem. Chem. Phys. 13 (2011) 207.
[33] L. Han, N. Koide, Y. Chiba, A. Islam, T. Mitate, C.R. Chim. 9 (2006) 645–651.
[34] L. Han, N. Koide, Y. Chiba, T. Mitate, Appl. Phys. Lett. 84 (2004) 2433.
[35] C.Y. Huang, Y.C. Hsu, J.G. Chen, V. Suryanarayanan, K.M. Lee, K.C. Ho, Sol. Energy Mater. Sol. Cells 90 (2006) 2391–2397.
[36] J.G. Chen, C.Y. Chen, S.J. Wu, J.Y. Li, C.G. Wu, K.C. Ho, Sol. Energy Mater. Sol. Cells 92 (2008) 1723–1727.
[37] T. Miyasaka, M. Ikegami, Y. Kijitori, J. Electrochem. Soc. 154 (2007) A455–A461.
[38] H.G. Yun, Y. Jun, J. Kim, B.S. Bae, M.G. Kang, Appl. Phys. Lett. 93 (2008) 133311.
[39] H.G. Yun, J.H. Park, B.S. Bae, M.G. Kang, J. Mater. Chem. 21 (2011) 3558.
[40] H.G. Yun, B.S. Bae, M.G. Kang, Adv. Energy Mater. 1 (2011) 337–342.
[41] Q. Wang, J.E. Moser, M. Grätzel, J. Phys. Chem. B 109 (2005) 14945–14953.
[42] T. Hoshikawa, M. Yamada, R. Kikuchi, K. Eguchi, J. Electrochem. Soc. 152 (2005) E68–E73.
[43] M. Wang, X. Li, H. Lin, P. Pechy, S.M. Zakeeruddin, M. Grätzel, Dalton Trans. (2009) 10015.
[44] S.Y. Huang, G. Schlichthörl, A.J. Nozik, M. Grätzel, A.J. Frank, J. Phys. Chem. B 101 (1997) 2576–2582.
[45] C. Shi, S. Dai, K. Wang, X. Pan, L. Zeng, L. Hu, F. Kong, L. Guo, Electrochim. Acta 50 (2005) 2597–2602.
[46] T.-Y. Cho, S.-G. Yoon, S.S. Sekhon, C.-H. Han, Bull. Korean. Chem. Soc. 32 (2011) 2058–2062.
[47] S. Kambe, S. Nakade, T. Kitamura, Y. Wada, S. Yanagida, 106 (2002) 2967–2972.
[48] J.E. Benedetti, M.A. De Paoli, A.F. Nogueira, Chem. Commun. (2008) 1121.
[49] K.C. Huang, R. Vittal, K.C. Ho, Sol. Energy Mater. Sol. Cells 94 (2010) 675–679.
[50] J.E. Benedetti, A.D. Gonçalves, A.L.B. Formiga, M.A. De Paoli, X. Li, J.R. Durrant, A.F. Nogueira, J. Power Sources 195 (2010) 1246–1255.
[51] G. Kalaignan, M. Kang, Y. Kang, Solid State Ionics 177 (2006) 1091–1097.
[52] A.I. Popov, R.F. Swensen, J. Am. Chem. Soc. 77 (1955) 3724–3726.
[53] L.Y. Lin, C.P. Lee, R. Vittal, K.C. Ho, J. Power Sources 195 (2010) 4344–4349.
[54] M.-H. Yeh, C.-P. Lee, L.-Y. Lin, P.-C. Nien, P.-Y. Chen, R. Vittal, K.-C. Ho, 56 (2011) 6157–6164.
[55] H.J. Snaith, A. Petrozza, S. Ito, H. Miura, M. Grätzel, Adv. Funct. Mater. 19 (2009) 1810–1818.